

# A Hierarchical Approach for Optic Disc Detection Using Wavelet Decomposition and Shape Based Pattern Classification

Sharath Kumar P N<sup>1</sup>, Deepak R U<sup>2</sup>, Midhun Raj R S<sup>3</sup>, Dr. Anuja Sathar<sup>4</sup>, Dr. Sahasranamam V<sup>5</sup>,  
Rajesh Kumar R<sup>6</sup>

Project Engineer, Health Informatics and Software Technology Group, Centre for Development of Advanced Computing, Thiruvananthapuram, India<sup>1</sup>

Senior Engineer, Health Informatics and Software Technology Group, Centre for Development of Advanced Computing, Thiruvananthapuram, India<sup>2</sup>

Graduate Apprentice, Health Informatics and Software Technology Group, Centre for Development of Advanced Computing, Thiruvananthapuram, India<sup>3</sup>

Assistant Professor, Department of Ophthalmology, Regional Institute of Ophthalmology, Thiruvananthapuram, India<sup>4</sup>

Professor, Department of Ophthalmology, Regional Institute of Ophthalmology, Thiruvananthapuram, India<sup>5</sup>

Principal Engineer, Health Informatics and Software Technology Group, Centre for Development of Advanced Computing, Thiruvananthapuram, India<sup>6</sup>

**Abstract:** Optic disc (OD) examination is of significant interest to both ophthalmologists and to image analysts. OD reveals symptoms of various ocular diseases like Glaucoma. For image analysts, optic disc detection although given its brighter intensities and sharp contrast is surprisingly a difficult task given its innumerable variations caused by retinal pathologies and imaging conditions. In this study, we propose a method for automatically detecting OD. The method involves a hierarchical approach where retinal image undergoes five-level wavelet decomposition for coarse OD detection which is followed by shape based classifier for precise OD boundary delineation. The proposed method was evaluated on 5789 images and achieved OD detection accuracy of 97.59%. OD boundary delineation performance was evaluated on a representative sample of 28 images and achieved a performance score of 88.37%. The results demonstrated consistency of the method across different image variations and can be adopted for various CAD applications on retinal images.

**Keywords:** automated detection, optic disc, wavelet decomposition, pattern classifier.

## I. INTRODUCTION

Optic disc (OD) is the portion of the optic nerve clinically visible on fundus examination of retina. Optic nerve is a cylindrical structure between retina and optic chiasm (see Fig. 1). Typically OD appears as a bright slightly oval structure with vertical diameter 9% greater than horizontal diameter with an average horizontal OD diameter of 1500 micrometers. Optic nerve which transmits visual information to brain leaves retina through OD. OD carries about 1 million neurons from the eye towards brain. OD is also called blind spot as it is not sensitive to light because of the absence of photosensitive rods and cones [1]. Examination of OD using fundus imaging (see Fig. 2) reveals symptoms of various diseases. Glaucoma, called as the silent thief of sight, is the third leading cause of blindness India. It can be detected by subtle variations of OD like optic cup to disc ratio, neuro-retinal rim, focal notching etc. OD borders can be blurred because of papilloedema or OD drusen. Color of the OD is also a

significant diagnostics feature. Healthy OD looks like an orange-pink ring with a pale center. Some diseases like advanced glaucoma, optic neuritis, arteritic or non-arteritic ischaemic optic neuropathy or a compressive lesion can cause the OD to appear pale.

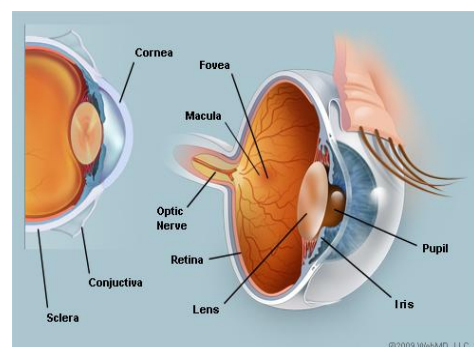


Fig.1. Anatomy of the eye

Thus optic disc shape, size and texture are important indicators of many ocular diseases [3]. In addition to direct diagnostic benefit, OD detection is considered as prerequisite for many of the computer aided diagnostic (CAD) algorithms. CAD is used for automated detection of retinal diseases and is considered to have a significant role in bridging enormous disparity between ophthalmologists to patient's ratio.

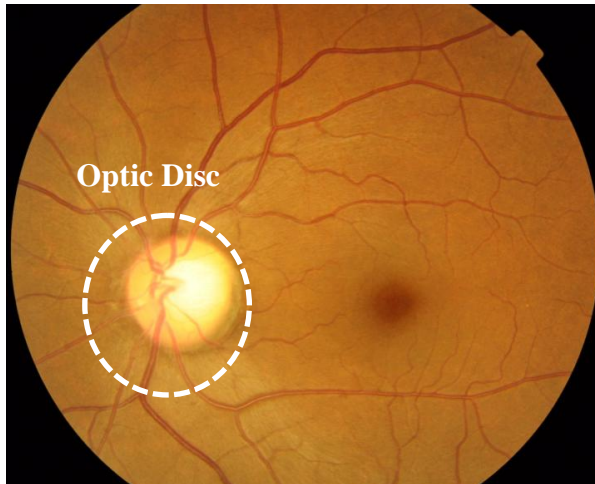


Figure 1: Retina imaged using fundus camera

Computer aided or automated OD detection is used for detection and tracking of retinal blood vessels which can predict various systemic diseases like diabetic retinopathy (DR), hypertensive retinopathy (HTR) and even heart disease or stroke [4]. OD detection is used for identifying another key retinal landmark, macula, responsible of central vision. Macula is located 2 disc diameter far from OD at an angle of  $17^\circ$  and this knowledge can be used as a priori information for automated localization of macula. CAD algorithms for automated detection of white lesions like exudates, drusen, cotton wool spots and Fibro Vascular Proliferations (FVP) can detect OD as false positives since it illustrates similar attributes to the white lesions in terms of color, brightness and contrast. By detecting OD, those false positives (FP) can be isolated from the true lesions [2-3]. Severity of ocular diseases is assessed based on the lesions on retinal quadrants which are centered on optic disc. Detection of optic disc is also required for identifying retinal quadrants.

Accurate OD detection despite its importance is not a trivial task as some parts of the boundary are not well defined while other parts are obscured by crossing blood vessels. OD itself has no uniform brightness where OD part on the nasal side is usually less bright than temporal side and occasionally not visible at all. Moreover, presence of pathological conditions such as exudates, FVP and peripapillary atrophy can hinder the success of the algorithm. Inconsistent image contrast, variability in appearance, uneven illumination can add up to challenges of automated OD detection.

Although there are numerous publications on optic disc localization few work without user intervention and only a still smaller subset accurately delineates OD boundary.

Work on automatic OD segmentation can be categorized into template matching methods, active contour/shape based methods and pixel classification based methods.

Template matching [5] method isolates OD by defining an OD template and matching it with different image locations. Image location which has strong correlation with template is considered to be OD. Although a straight forward and flexible template matching is a computationally expensive operation. Another major drawback is that template matching need not always result in an accurate OD boundary delineation. Notable work has been done by Aquino et al. [6], Wong et al. [7], Zheng et al. [8], Giachetti et al. [9] using template matching based methods. Active contour/shape [10] based models or snakes delineate OD boundary precisely by detecting the presence of edge by assessing continuity, curvature combined with local edge strength. Snakes interpolate missing edges of OD caused by blood vessels, while retaining visible edges. On the downside initial contour of the snake must be close to the desired boundary otherwise success of these methods is dependent on convergence criteria used in the energy minimization technique. Notable works in this category are done by Lowell et al. [11], Xu et al. [12], Li and Chutatape [13], Joshi et al. [14] and Hsiao et al. [15]. Pixel classification method used supervised or non-supervised machine learning techniques to classify each pixel as either belonging to an OD or not by relying on set of mathematical features derived from intensity, texture, relationship to neighbouring pixels etc. Although this method reduces the bias compared to other categories which relies on one or two features. On the other hand, OD boundary delineation accuracy need to be further studied. Notable works in this category are done by Abramoff et al. [16] and Cheng et al. [17]. In the proposed work we followed a hierarchical approach based on wavelet decomposition followed by shape based pattern classification which results in high accuracy OD detection without compromising in OD boundary delineation.

## II. MATERIALS

### A. Data Collection

Site 1 - A dataset of 4047 retinal images from 1190 diabetic patients were obtained from the DR diagnosis program at the Regional Institute of Ophthalmology (RIO), Thiruvananthapuram. In the DR diagnosis program, 2380 patient retinas were screened by the ophthalmologists. The retinal images were nominally 500 field-of-view acquired using Topcon TRC-50DX mydriatic fundus camera with Nikon D90 DSLR camera. The resulting color images were 3.1 megapixels with image size being 2144 X 1424 pixels. All the images were stored using lossless TIFF compression. All patients underwent routine mydriasis with Tropicamide 1% and both eyes were imaged. Two image fields per eye were taken: a fovea-centred and a disc-centred view.

Site 2 - A dataset of 1742 retinal images from 761 diabetic patients were obtained from the DR diagnosis program at the Indian Institute of Diabetes (IID), Thiruvananthapuram. In the DR diagnosis program, 1522

patient retinas were screened by the ophthalmologists. The retinal images were nominally 450 field-of-view acquired using Topcon TRC-NW8F mydriatic fundus camera with Nikon D90 DSLR camera. The resulting color images were having image sizes 3216 X 2136, 2574 X 1710 and 2188 X 1454 pixels. All the images were stored either as lossless TIFF or as lossy JPEG compression. All patients underwent routine mydriasis with Tropicamide 1% and both eyes were imaged. One image field per eye were taken: a fovea-centred view. Images obtained from the two deployment sites were used for this study after getting clearance from the human ethics committee vide letter no. 32/HEC/RIOTVPM dated 16/10/2014.

**B. Manual Image Grading**

Images from all the patients were annotated and independently marked by a team of two ophthalmologists at RIO (T) according to the Early Treatment Diabetic Retinopathy Study [18]. For the annotations, ophthalmologists were provided with Retinal Image Annotation and Grading Software (RIAG) developed by the authors. Using the software, ophthalmologists marked optic disc and assessed image quality as either good or average or poor for 5789 images. A randomly selected representative sample of 28 images’ OD boundary was marked by Ophthalmologists. Ophthalmologist’s identification of OD and its boundaries were used as ground truth for calculating OD detection accuracy and OD boundary delineation performance respectively.

**III.METHODS**

The flow chart of the proposed OD detection method is depicted in the Fig. 3. The retinal images obtained from Site 1 and 2 were used for the detection of OD.

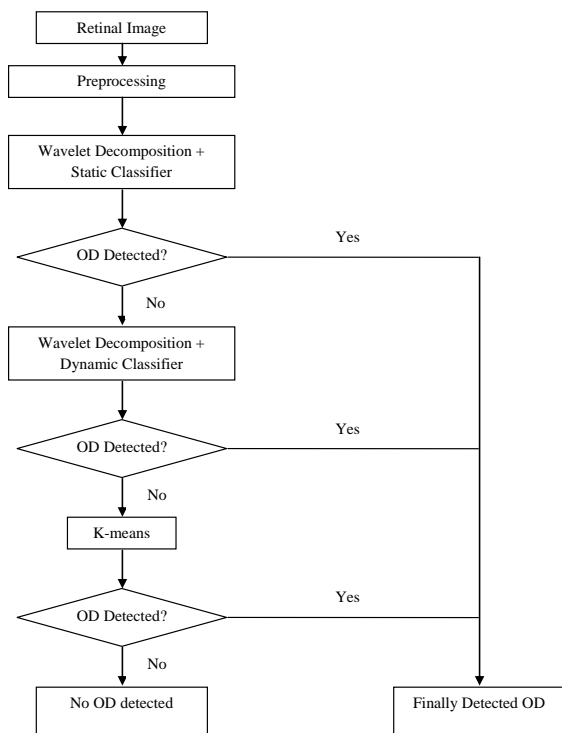


Fig3. Flow chart of the proposed OD detection

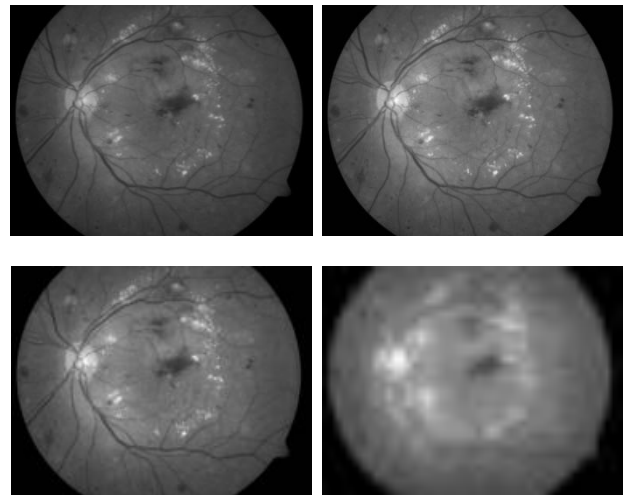


Fig. 4. Wavelet Decomposition. (a) Green channel of the retinal image. (b) Image at first level. (c) Image at third level. (d) Image at fifth level. At this level, only few bright pixels fall into the original OD region

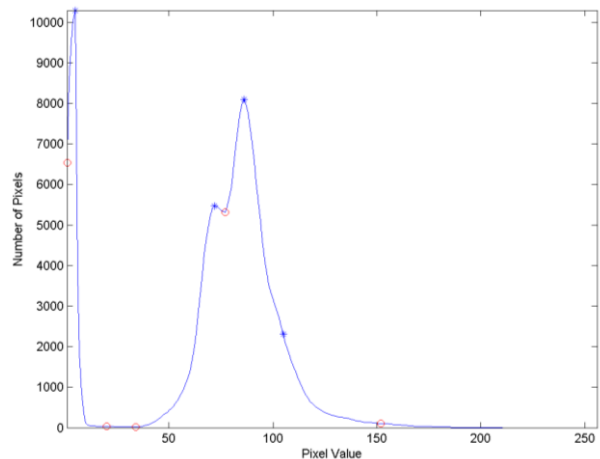


Fig5. Histogram of the green channel image

**Prior Knowledge:** Here, we have utilized three important features about OD in the retinal image. Firstly, exploiting the structure of the retina while capturing the retinal image using fundus camera. Optometrist knows which eye is being imaged and whether the image is a fovea centered or disc centered. This information is encoded in the image nomenclature and thus helps to search OD in a specific portion of the image. Secondly, observations from the retinal image histogram which signifies OD as bright region in the retinal image. Thirdly, OD appears circular in shape.

**Wavelet Decomposition:** OD is the bright yellowish region and has the highest contrast with the background in the green channel image [19]. Hence, green channel image is used as the starting point in our proposed method. Here, we utilize the advantage of the wavelet decomposition by obtaining different low level resolution images. Fig. 4 shows the green channel of original RGB image and its low level resolution images. From our experimental analysis, we chose the low resolution image obtained at the fifth level of wavelet decomposition. From the Fig. 4



(d) it is evident that only few bright pixels fall into the original OD region. Because of the small image size at the lowest resolution, small bright regions (such as white lesions like exudates and cotton-wool spots) vanish. For the implementation efficiency, the low resolution image is obtained using Haar wavelet with [-1, 1] and [1, 1] as high-pass and low-pass filters respectively [20]. Potential OD regions are extracted from this method.

**Binary Thresholding:** Binary thresholding is performed on the decomposed image by choosing appropriate intensity value as threshold which is obtained from the histogram analysis [21]. According to the author, the intensity profile of the retinal image starts with dark (red) lesions (microaneurysms and haemorrhages); secondly the blood vessels which are not as dark as red lesions; next is bright (white) lesions which appear yellowish in color and lastly the brightest being the OD. They have found that in the intensity distribution of retinal image, there are four distinct peaks corresponding to four regions with first peak for red lesions and last peak for OD as shown in Fig. 5. Here, we chose static threshold in the first level OD detection and dynamic threshold in the second level OD detection which is obtained from the histogram analysis. From this, potential OD candidates are obtained.

**Region Growing:** Firstly, seed for each of the potential OD candidates are obtained from the binary image. Region is grown on the seed by combining adjacent areas whose Euclidean distance falls below experimentally chosen value. This process is continued until the point where no more regions can be grown. Here, we also restrict the region growing on the seeds which does not fall in the search area of the binary image mentioned under first prior knowledge section.

**Classification:** From the third prior knowledge, it is said that OD appears in circular shape. In the first level OD detection, we classify only those OD candidate which exactly circular in shape. To do this, a classification model is created with the help of two shape features namely eccentricity and solidity. In the second level OD detection, we classify those OD candidate which appropriately (not exactly circular) circular in shape. To bring variation in the classifier model, we added two more features namely compactness and circularity. In the third level OD detection, we used k-means clustering method to identify OD. Here, based on the second prior knowledge we chose the 5th cluster to detect OD.

#### A. Preprocessing of Retinal Images

Retinal images obtained from Site 1 and 2 were used for detection of OD. Images from two sites were having different resolutions. To make OD detection consistent on all the resolutions, scale of the images were first standardized to 1500 X 1000 pixels which will also make the OD detection computationally efficient.

#### B. First-level OD Detection Using Wavelet Decomposition and Pattern Classification

The procedure we use goes as follows

- 1) Convert the original RGB image into grayscale image by choosing green channel image [19];

- 2) Extract potential OD regions by performing five-level wavelet decomposition [19] on the green channel image using Haar wavelet with [1,-1] and [1,1] as high-pass and low-pass filters respectively [20];
- 3) A static threshold ( $T = 200$ ) was experimentally chosen based on the 2<sup>nd</sup> prior knowledge;
- 4) Apply binary thresholding using  $T$  on the decomposed image to obtain potential OD candidates;
- 5) Extract seed for each of the OD candidates;
- 6) Perform region growing using extracted seed for each of the OD candidates [1<sup>st</sup> prior knowledge];
- 7) Classify the region grown OD candidates as actual OD using two shape features [3<sup>rd</sup> prior knowledge].

#### C. Second level OD Detection Using Wavelet Decomposition and Pattern Classification

The procedure we use as follows

- 1) Convert the original RGB image into grayscale image by choosing green channel image [19];
- 2) Extract potential OD regions by performing five-level wavelet decomposition [19] on the green channel image using Haar wavelet with [1,-1] and [1,1] as high-pass and low-pass filters respectively [20];
- 3) Derive a dynamic threshold value from the histogram analysis [21];
- 4) Apply binary thresholding on the decomposed image to obtain potential OD candidates;
- 5) Extract seed for each of the OD candidates;
- 6) Perform region growing using extracted seed for each of the OD candidates [1<sup>st</sup> prior knowledge];
- 7) Classify the region grown OD candidates as actual OD using four shape features [3<sup>rd</sup> prior knowledge].

#### D. Third level OD Detection Using K-means clustering

The procedure we use as follows

- 1) Convert the original RGB image into grayscale image by choosing green channel image [19];
- 2) Extract potential OD regions by performing k-means clustering on the green channel image;
- 3) Obtain potential OD candidates by choosing fifth cluster based on the 2<sup>nd</sup> prior knowledge;
- 4) Perform circle fitting using shape features.

## IV. RESULTS AND DISCUSSION

A dataset of 5789 images obtained from 1951 patients from Site 1 and 2 were used for this study. All the images analyzed using the automated OD detection method proposed here, were compared against ground truth provided by the ophthalmologists. Accuracy of the proposed method was measured using True Positive (TP), True Negative (TN), False Positive (FP) and False Negative (FN) which is defined by equation (1). OD detection accuracy of the proposed hierarchical method was 97.59%. The method achieved an OD detection accuracy of ~78% in the first-level, ~16% in the second-level and ~3% in the third level.

$$\text{Accuracy} = \frac{TP+TN}{TP+TN+FP+FN} \quad (1)$$

OD boundary delineation performance was evaluated using OD boundary marked by domain expert (G) and OD detected by the proposed method (D) which is defined by equation (2). The proposed hierarchical method achieved a performance score (S) of 88.37%.

$$S = \frac{\text{Area (G \cap D)}}{\text{Area (G \cup D)}} \quad (2)$$

Table I shows the accuracy of the proposed method for the two deployment sites. As the camera field-of-view is different for the two sites, the detection of OD becomes harder. Since our proposed method is independent of size, the detection of OD remains efficient. Also, our OD detection was tested against different resolution images with varying intensities and retinal pathologies. This makes our method robust enough to identify OD with wide image variations. Hence, from Table I it is evident that independent of the image resolution and camera field-of-view our proposed method was efficient in detecting OD

accurately. Another major challenge in detection of OD is presence of pathologies like exudates which mimics the intensity characteristics of OD. Proposed method made use of shape based pattern classifier for distinguishing OD from exudates.

In the Table II, we have presented the performance score (S) of the proposed method for a representative sample of 28 images along with the image quality as perceived by the ophthalmologist. As it is evident from the Table II, the proposed method had shown consistent performance irrespective of the image qualities like Good, Average and Poor (see Fig. 6, 7 and 8 respectively). In Table II, we have also included images where OD is obscured by retinal pathologies like FVP, images suffering from low contrast, blurred, and uneven illumination of image or within OD. All such images are categorized as ‘Poor’. Although, there is a marginal dip in performance (S) for ‘Poor’ images, the proposed method was able to accurately detect OD (see Fig. 8).

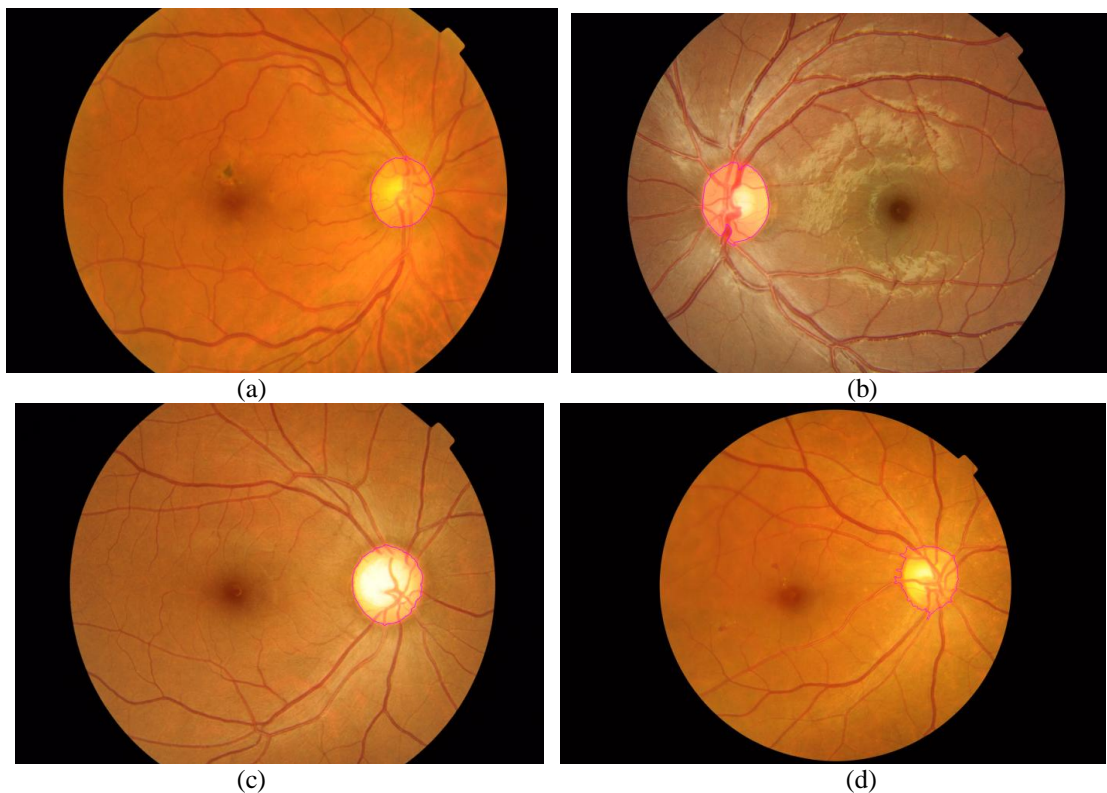


Fig. 6 Results of OD Detection (a-d) Good quality images

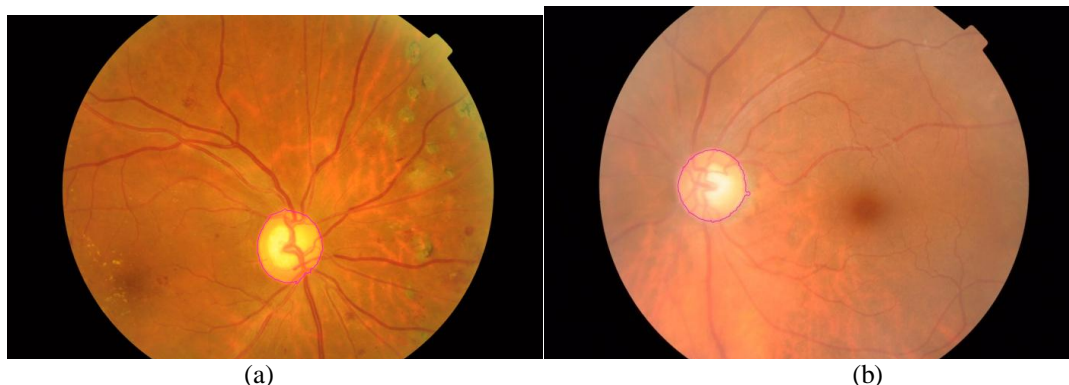


Fig. 7. Results of OD Detection. (a-b) Average quality images with incomplete temporal arcades.

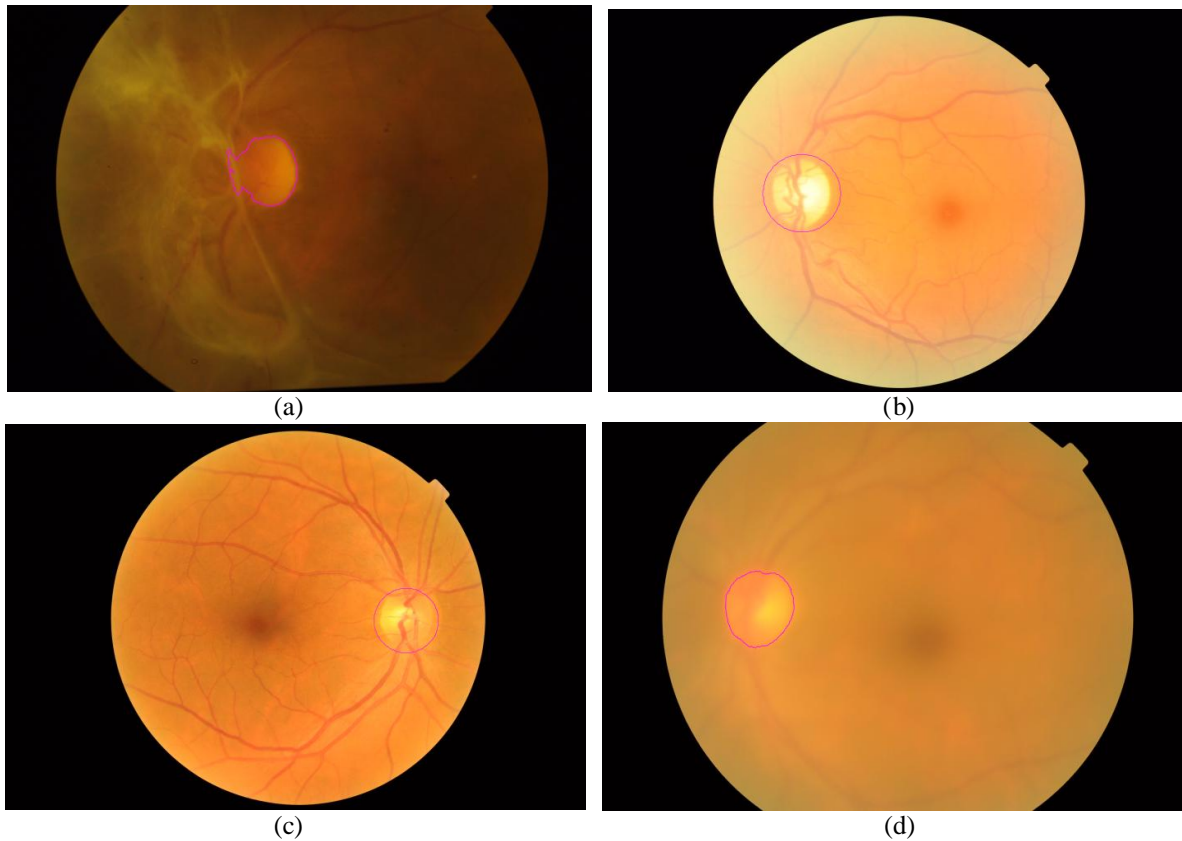


Fig 8 Results of OD Detection Poor quality images with (a) FVP. (b) Glare. (c) Uneven illumination within OD. (d) Poor OD boundary.

Table I Accuracy Details

Deployment Site	Camera Field-of-View	Image Resolution	Count of Retinal Images	Accuracy (%)
1	500	2144 X 1424	4047	97.38
2	450	3216 X 2136, 2574 X 1710, 2188 X 1454	1742	98.1

Table II Performance Details

Image	Ground Truth	S (%)
001_L_1	Good	92.78
002_R_1	Good	73.21
003_R_2	Good	94.15
004_R_1	Good	90.75
005_L_1	Good	82.35
006_R_2	Good	93.5
007_R_1	Good	92.42
008_R_2	Good	93.15
009_R_1	Good	93.58
010_R_1	Good	94.84
011_R_2	Good	90.93
012_L_2	Good	93.76
013_R_1	Good	96.29
014_L_1	Good	91.63
015_L_2	Good	88.23
016_R_2	Good	94.08
017_R_1	Good	87.62
018_L_1	Good	91.38
019_L_2	Good	86.09



020_R_1	Good	90.04
021_L_1	Average	91.55
022_L_1	Average	91.55
023_R_2	Average	95.79
024_L	Poor	63.35
025_R	Poor	70.75
026_R	Poor	77.79
027_L_1	Poor	86.91
028_L_2	Poor	85.81

**V. CONCLUSION**

In this study, we have presented a hierarchical approach for OD detection based on wavelet decomposition followed by shape based pattern classification. The proposed method was validated against expert ophthalmologist’s ground truth. The proposed method was evaluated on 5789 images and achieved an accuracy of 97.59%. OD boundary delineation performance evaluation demonstrated accurate delineation of OD boundary and achieved a performance score of 88.37%.

The results show that the proposed method can be adopted for various CAD applications on retinal images. The method has direct relevance in detecting diseases like Glaucoma which demands OD detection accuracy and precise OD boundary delineation. Additionally the proposed method can also be used to identify retinal anatomical structures like macula/fovea. This method can also be used for reducing false positives in CAD application on retinal images.

**ACKNOWLEDGMENT**

We acknowledge the Department of Electronics and Information Technology (DeitY) for the financial support. Also, we would like to thank The Department of Ophthalmology, Regional Institute of Ophthalmology (RIO), Thiruvananthapuram and Indian Institute of Diabetes (IID) who provided us with the required set of fundus images. The ophthalmologists and domain experts from RIO and IID were consulted for gaining domain knowledge and for the verification and establishment of ground truth for this study.

**REFERENCES**

[1] <http://www.optic-disc.org/>  
 [2] B. Dashtbozorg, A. M. Mendonça, A. Campilho, “Optic Disc Segmentation using the sliding Band Filter,” *Computers in Biology and Medicine*, vol. 56, pp. 1-12, 2015. DOI: 10.1016/j.combiomed.2014.10.009.  
 [3] Jelinek H.F., Cree M.J.. *Book on Automated Image Detection of Retinal Pathology*. ISBN 978-0-8493-7556-9.  
 [4] Downie et.al. Hypertensive retinopathy: comparing the Keith-Wagener-Barker to a simplified classification. *J Hypertens*. 2013 May;31(5):960-5. doi: 10.1097/HJH.0b013e32835efea3.  
 [5] R. Brunelli, *Template Matching Techniques in Computer Vision: Theory and Practice*, Wiley, ISBN 978-0-470-51706-2, 2009.  
 [6] Arturo Aquino, Manuel Emilio Gegúndez-Arias, and Diego Marín. Detecting the optic disc boundary in digital fundus images using morphological, edge detection, and feature extraction techniques. *IEEE Trans. Med. Imag.*, 29(11):1860–1869, 2010.  
 [7] DWK Wong, J Liu, JH Lim, X Jia, F Yin, H Li, and TY Wong. Level-set based automatic cup-to-disc ratio determination using

retinal fundus images in ARGALI. In *Engineering in Medicine and Biology Society, 2008. EMBS 2008. 30th Annual International Conference of the IEEE*, pages 2266–2269. IEEE, 2008.  
 [8] Yuanjie Zheng, Dwight Stambolian, Joan O’Brien, and James C Gee. Optic disc and cup segmentation from color fundus photograph using graph cut with priors. In *Medical Image Computing and Computer-Assisted Intervention–MICCAI 2013*, pages 75–82. Springer, 2013.  
 [9] Andrea Giachetti, Lucia Ballerini, and Emanuele Trucco. Accurate and reliable segmentation of the optic disc in digital fundus images. *Journal of Medical Imaging*, 1(2):024001–024001, 2014.  
 [10] Kass, M.; Witkin, A.; Terzopoulos, D. (1988). "Snakes: Active contour models" (PDF). *International Journal of Computer Vision* 1 (4): 321. doi:10.1007/BF00133570.  
 [11] James Lowell, Andrew Hunter, David Steel, Ansu Basu, Robert Ryder, Eric Fletcher, and Lee Kennedy. Optic nerve head segmentation. *Medical Imaging, IEEE Transactions on*, 23(2):256–264, 2004.  
 [12] Juan Xu, Opas Chutatape, Eric Sung, Ce Zheng, and Paul Chew Tec Kuan. Optic disk feature extraction via modified deformable model technique for glaucoma analysis. *Pattern recognition*, 40(7):2063–2076, 2007.  
 [13] Huiqi Li and Opas Chutatape. Automated feature extraction in color retinal images by a model based approach. *Biomedical Engineering, IEEE Transactions on*, 51(2):246–254, 2004.  
 [14] G Joshi, Jayanthi Sivaswamy, and SR Krishnadas. Optic disk and cup segmentation from monocular color retinal images for glaucoma assessment. *Medical Imaging, IEEE Transactions on*, 30(6):1192–1205, 2011.  
 [15] Hung-Kuei Hsiao, Chen-Chung Liu, Chun-Yuan Yu, Shiao-Wei Kuo, and Shyr-Shen Yu. A novel optic disc detection scheme on retinal images. *Expert Systems with Applications*, 39(12):10600–10606, 2012.  
 [16] Michael D Abramoff, Wallace LM Alward, Emily C Greenlee, Lesya Shuba, Chan Y Kim, John H Fingert, and Young H Kwon. Automated segmentation of the optic disc from stereo color photographs using physiologically plausible features. *Investigative ophthalmology & visual science*, 48(4):1665–1673, 2007.  
 [17] Jun Cheng, Jiang Liu, Yanwu Xu, Fengshou Yin, Damon Wing Kee Wong, Ngan-Meng Tan, Dacheng Tao, Ching-Yu Cheng, Tin Aung, and Tien Yin Wong. Superpixel classification based optic disc and optic cup segmentation for glaucoma screening. *Medical Imaging, IEEE Transactions on*, 32(6):1019–1032, 2013.  
 [18] Fundus photographic risk factors for progression of diabetic retinopathy. ETDRS report number 12. Early Treatment Diabetic Retinopathy Study Research Group. *Ophthalmology*, vol. 98, no. 5, pp. 823-833, 1991.  
 [19] M. Lalonde, M. Beaulieu and L. Gagnon, "Fast and robust optic disc detection using pyramidal decomposition and hausdorff-based template matching", *IEEE Trans. Medical imaging*, vol. 20, no. 11, pp.1193-1200, 2001.  
 [20] S. G. Mallat, "A theory for multiresolution signal decomposition: The wavelet representation", *IEEE Trans. Pattern Anal. Machine Intell.*, vol. 11, pp.674-693, 1989.  
 [21] Sharath Kumar P N, Rajesh Kumar R, Anuja Sathar, Sahasranamam V, “Automatic Detection of Exudates in Retinal Images Using Histogram Analysis,” in *IEEE International Conference on Recent Advances in Intelligent Computational Systems (RAICS)*, pp. 277-281, December 2013.